Group-IIIA versus IIIB delafossites: Electronic structure study

Muhammad N. Huda,* Yanfa Yan, Aron Walsh, Su-Huai Wei, and Mowafak M. Al-Jassim
National Renewable Energy Laboratory, Golden, Colorado 80401, USA

(Received 3 March 2009; revised manuscript received 7 May 2009; published 23 July 2009)

First-principles density-functional theory calculations reveal significantly different behavior between group-IIIA and IIIB delafossites CuMO$_2$. The group-IIIA delafossites have indirect band gaps with large differences between the direct and indirect band gaps. However, this difference is small for the group-IIIB delafossites: only 0.22 eV for $CuScO_2$ and it diminishes further for $CuYO_2$ and $CuLaO_2$. Also, whereas group IIIA prefers rhombohedral stacking, group IIIB stabilizes in hexagonal structures. We further find that $CuScO_2$ has the highest calculated fundamental band gap among all the delafossite oxides. In addition, $CuLaO_2$ is found to have a direct band gap. These differences are explained by the different atomic configurations between the group-IIIA and IIIB elements. Our understanding of these delafossites provides general guidance for proper selection of delafossites for suitable applications in optoelectronic devices.

DOI: 10.1103/PhysRevB.80.035205 PACS number(s): 71.20.−b, 78.20.−e, 71.15.Mb

I. INTRODUCTION

Cu delafossites, CuMO$_2$ (M=group III elements), have received great attention in recent years due to their potential applications as electrodes for hydrogen production by photoelectrochemical (PEC) water splitting and transparent conductive oxides (TCOs) in optoelectronic devices.[1–8] It is the p-type conductivity and good hole mobility that make the Cu delafossites so unique and more attractive in these applications than other metal oxides. For instance, due to their p-type nature, the Cu delafossites are resistive against oxidative corrosion. Some recent experimental studies demonstrated that Cu delafossites are stable in solution and are capable of H_2 evolution from water.[6,7] For the application of TCOs, the currently available TCOs, such as ZnO, In_2O_3:Sn, or In_2O_3:Mo, are mostly n-type; hence, their use is limited for transparent p-n semiconductor devices.[9,10] The realization of p-type conductivity and good hole mobility in Cu delafossites is because their valence-band maximum (VBM) is composed of hybridized Cu d and O p antibonding orbitals.[11]

Among the two Cu delafossites families, [CuM^{IIIA}O$_2$ (M^{IIIA}=Al, Ga, and In) and CuM^{IIIB}O$_2$ (M^{IIIB}=Sc, Y, and La)], the CuM^{IIIA}O$_2$ family (particularly, M^{IIIA}=Al) has mostly been considered for p-type TCOs, although a later theoretical study[12] has revealed that this delafossite family does not exhibit direct band gaps. Their fundamental band gaps, i.e., from VBM to conduction-band minimum (CBM) could be significantly smaller than their reported optical band gaps. On the other hand, the CuM^{IIIB}O$_2$ family may also be used as good p-type TCO materials; however, the focus on this family has so far been limited and specifically on the application on H production by solar water splitting. Until now, there is no solid understanding on which family is better suited for a particular application. Despite the similar structures, the CuM^{IIIA}O$_2$ and CuM^{IIIB}O$_2$ families exhibit significantly different electronic properties. The optical measurements indicate that the group-IIIA delafossite family has indirect band gaps.[13,14] Also, these can hardly be doped p-type by extrinsic dopants.[15,16] On the other hand, the group-IIIB delafossites family has been exclusively reported to have direct wide band gaps and can be doped by extrinsic dopants.[6,7] It has been reported previously that the CuM^{IIIA}O$_2$ family shows band-gap anomalies with respect to other group-III-containing semiconductors: the measured optical band gap increases from 3.5 eV ($CuAlO_2$) to 3.6 eV ($CuGaO_2$) to 3.9 eV ($CuInO_2$) (Ref. 12) while they decrease for the corresponding binary oxides and nitrides. However, the group-IIIB delafossite family, CuM^{IIIB}O$_2$, does not show such anomalies and exhibits a totally opposite band-gap trend. The measured band gap decreases from 3.7 eV ($CuScO_2$) (Ref. 17) to 3.5 eV ($CuYO_2$) (Ref. 18) to 2.4 eV ($CuLaO_2$).[19] It is also important to note that the main difference between the requirements for PEC electrodes and TCOs is that the former require smaller band gaps (in the visible region) and an appropriate band-edge alignment, whereas the later require larger band gaps (in the ultraviolet region). Therefore, a detailed comparative study needs to be conducted on the electronic structure between the CuM^{IIIA}O$_2$ and CuM^{IIIB}O$_2$ families so that these materials can be used for their best-suited applications in optoelectronic devices. However, to date, the nature of the band gaps of the CuM^{IIIB}O$_2$ family is still not well understood and needs to be examined carefully and systematically.

In this paper, we systematically examine the structural stability and electronic structure of CuM^{IIIB}O$_2$ delafossites using density-functional theory (DFT) and compare them with their sister system, CuM^{IIIA}O$_2$ delafossites. We provide a detailed understanding on why and how these two Cu delafossite families exhibit different electronic structures. We find that these two delafossite families behave differently, largely due to the different crystal structures and electronic configurations for group-IIIA and IIIB cations. The differences can be summarized as: (i) the CuM^{IIIA}O$_2$ family prefers rhombohedral symmetry, whereas the CuM^{IIIB}O$_2$ family prefers the hexagonal symmetry; (ii) the CuM^{IIIA}O$_2$ family produces indirect band gaps with large differences between the direct and indirect band gaps. However, for group IIIB this difference is very small; for $CuScO_2$ it is 0.22 eV and diminishes further for $CuYO_2$ and $CuLaO_2$. (iii) The band-gap anomalies observed in the CuM^{IIIA}O$_2$ family are not found in CuM^{IIIB}O$_2$. Direct band gaps of group-IIIB delafossites are examined carefully here because the indirect gaps

are so prominent in their sister-group delafossites. This understanding would provide a solid mechanism to design and engineer the band-gap properties of these delafossite oxides for commercial optoelectronic devices. Our results suggest that $CuScO_2$ and $CuYO_2$ delafossites may be better *p*-type TCO candidates than $CuM^{IIIA}O_2$ delafossites. On the other hand, given the smaller band gap, $CuLaO_2$ would be more suitable for PEC photoelectrode application than other Cu delafossites.

II. METHODS

We have employed DFT to study the electronic properties of the delafossites materials. Generalized gradient approximation (GGA) to DFT (Ref. 20) and the projected augmented wave basis[21,22] as implemented in the Vienna *ab initio* simulation package[23] are used. Plane-waves cutoff energy of 400 eV was used and the ion positions were always relaxed until the force on each of them is 0.01 eV/Å or less. Depending on the supercell, as will be discussed below, we have used $13\times13\times13$ (rhombohedral cell) and $13\times13\times3$ (for hexagonal cell) *k*-point distribution for the final energy calculations. To correct the DFT-GGA underestimation of electron correlation in the cation *d* bands, DFT+*U* method has been used. It should be noted that the choice of the *U* parameters cannot be determined uniquely within the present methodology. So a range of *U* values were examined to check their effect on the delafossites. Although a larger *U* parameter can open up the band gap further, it also affects the volume. So a compromise is necessary. For the results reported in this paper, an U_{eff}(*U*-*J*=7 eV) parameter was added to the DFT Hamiltonian for all the valence Cu *d*, Sc *d*, and Y *d* bands. No *U* was added for the group-IIIA elements because their filled 3*d* bands are fully occupied shallow core states, which are situated more than 15 eV below the top of the valence band (Al has no occupied *d* band). It has also been found that adding an additional *U*, for example, on the Ga 3*d* band resulted in a much smaller in-plane lattice *a* parameter compared to the experimental value. In the case of $CuLaO_2$, an empty and highly localized *f* band is present just above the CBM and a localized band with *d* character is seen in the lower edge of the conduction band. This overall presence of *f* on top of *d* character at the CBM makes it particularly sensitive on the choice of *U* parameter in the DFT+*U* scheme. In fact, we have found that a small *U* value on the La *d* band highly overestimates the band gap relative to experiment. So, for $CuLaO_2$, no *U* potential has been used to La 5*d*. The choice of *U* parameter was not found to affect the relative stability of the hexagonal and rhombohedral delafossite structures. These choices of *U* give the experimental band-gap trend for the group-IIIB delafossites. Further justification and discussion on the choice of *U* parameter will be presented in Sec. III C where the band-gap trend of these two delafossite families will be discussed.

III. RESULTS AND DISCUSSIONS

We first discuss the structure preferences for the group-IIIA and IIIB delafossites. The delafossite structure can have either $P6_3/mmc$ (#194) or $R\bar{3}m$ (#166) space-group symmetry depending on the stacking sequencing of the O–*M* (*M* =group IIIA and IIIB) octahedron layers, as shown in Fig. 1. Both the hexagonal [Fig. 1(a)] and rhombohedral cell [Fig. 1(b)] are shown in their conventional unit cell to compare. For the hexagonal cell, two stacking units are shown. These two units are then periodically repeated in all three directions. For the rhombohedral cell, the lower two stacking units are similar to the hexagonal cell; however, the top unit has a different stacking pattern than the hexagonal cell. These three units are then repeated periodically in all directions for the rhombohedral cell. $CuAlO_2$ is experimentally recognized to be in the rhombohedral group ($R\bar{3}m$) with one formula unit (four atoms) per primitive cell and three formula units per conventional unit cell [as shown in Fig. 1(b)], whereas $CuYO_2$ has been reported to be in the hexagonal group ($P6_3/mmc$) with two formula units per cell.[24] In both symmetries, O and Cu form a linear bonding structure along the *c* axis, which is considered to be the main channel for the hole transport, whereas O–*M* bonds form distorted octahedra.

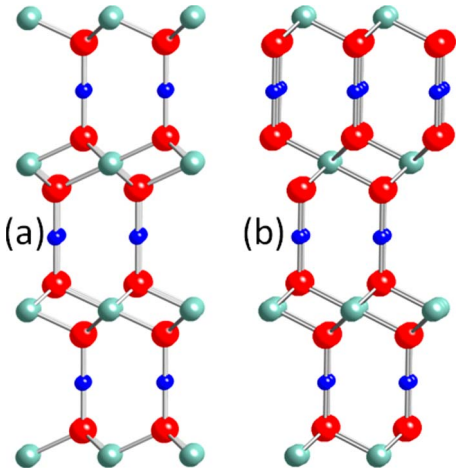

FIG. 1. (Color online) (a) Hexagonal and (b) rhombohedral stacking of the delafossite structures are shown here. The red (large balls) and blue (small balls) are oxygen and copper atoms, respectively. The light green atoms (medium balls) are group-IIIA or IIIB cations.

The calculated lattice constants for both the rhombohedral and hexagonal unit cells agree well with the available experimental values. The calculated lattice constants for various delafossites are shown in Table I. For example, for hexagonal $CuYO_2$, we found $a=3.628$ Å and $c=11.420$ Å, whereas the experimental values are $a=3.521$ Å and $c=11.418$ Å.[23] For the conventional rhombohedral unit cell, our calculated lattice constants correspond to $a=3.521$ Å and $c=17.178$ Å. The longer *c* in rhombohedral unit cell corresponds to the different stacking sequence of the metal-oxide octahedron layers along the *z* direction. However, when normalized per formula unit (i.e., one stacking height), the hexagonal and rhombohedral *c* values become $c/2=5.709$ Å and $c/3=5.726$ Å, respectively. The energy per formula unit for the hexagonal structure for $CuYO_2$ is lower by 0.034 eV than the rhombohedral structure. These differences are 0.050

TABLE I. Calculated lattice constants a and c (in Å) for the conventional unit cell in hexagonal (Hex) and rhombohedral (Rhom) structures for the delafossites. The formation energy difference ΔH_f (in eV) is relative to the ground-state structures.

	Hex		Rhom		ΔH_f	
Delafossite	a	c	a	c	Hex	Rhom
$CuAlO_2$	2.849	11.355	2.845	17.025	0.027	0
$CuGaO_2$	2.976	11.419	2.973	17.114	0.006	0
$CuInO_2$	3.196	11.544	3.301	17.404	0.002	0
$CuScO_2$	3.308	11.372	3.180	17.190	0	0.050
$CuYO_2$	3.628	11.402	3.521	17.178	0	0.034
$CuLaO_2$	3.813	11.355	3.800	16.981	0	0.015

and 0.015 eV per formula unit for $CuScO_2$ and $CuLaO_2$, respectively. On the other hand, the group-IIIA delafossites prefer the $R\bar{3}m$ structure. For example, the energy per formula unit for $CuAlO_2$ structure in $R\bar{3}m$ symmetry is 0.027 eV lower than the hexagonal structure. For $CuGaO_2$ and $CuInO_2$, this difference is 0.006 and 0.002 eV, respectively, which may fall within the accuracy limit of DFT calculations. The calculated lattice constants, for example, for rhombohedral $CuAlO_2$ are $a=2.845$ Å and $c=17.025$ Å, and they compare well with the previous DFT calculations and with the experimental values.[8] However, it should be pointed out that because the energy differences between the rhombohedral and hexagonal structures are small, it is possible that the synthesized materials may exhibit either of these two symmetry groups or mixed structures, depending on the growth conditions.

A. Density of states

From Fig. 1 and our discussion above, one can see that the rhombohedral and hexagonal delafossites differ only in stacking sequence, and the local bonding environments are similar. So, it may be expected that a given delafossite in these two structures may have similar electronic features. It has been reported previously, in the case of Cu(I)-based cuprous oxide, that the VBM is composed of hybridized Cu d and O p antibonding states.[11,25] So, for the two families of delafossites, this antibonding VBM is expected to be a common feature. The antibonding nature of the valence-band edge is the main reason for the relatively higher mobility of holes, compared to the other oxides (such as ZnO). Figure 2 shows the calculated total electronic density of states (DOS) plot for three representative delafossites: (a) $CuAlO_2$, (b) $CuGaO_2$, and (c) $CuScO_2$ in both hexagonal and rhombohedral symmetries. The reason to have the $CuAlO_2$ DOS plot (which has no occupied d band contribution from Al) is to compare with $CuGaO_2$ (which has filled $3d$ band from Ga). On the other hand, for Sc(III), the $3d$ band is located in the conduction band. Fermi energy is defined here as the top of the valence band and the energies are scaled with respect to $E_f=0.00$ eV. The overall features of the DOS plots are almost the same within the same group of delafossites. The electronic difference between the two groups is mostly

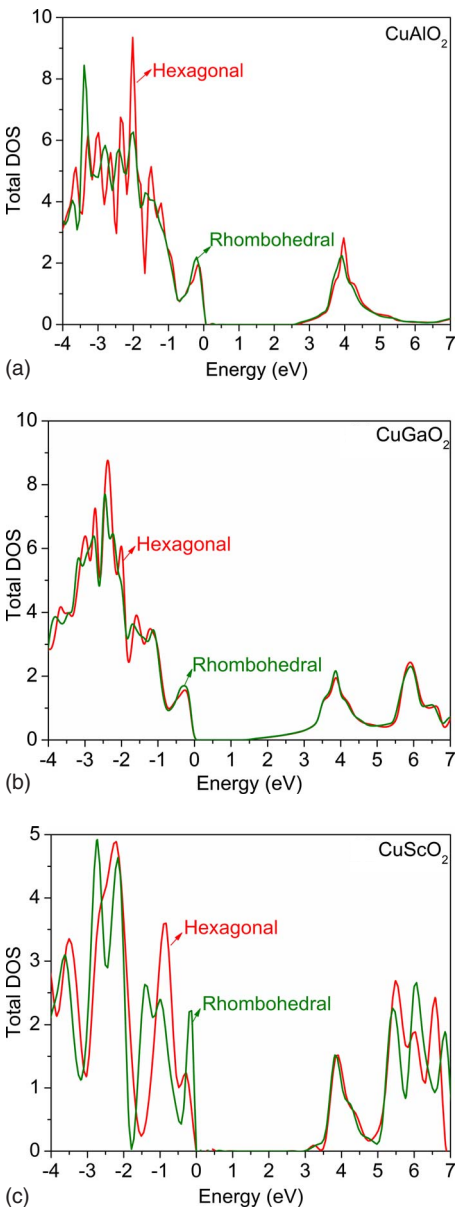

FIG. 2. (Color online) Total electronic densities of states for (a) $CuAlO_2$, (b) $CuGaO_2$, and (c) $CuScO_2$ in $P6_3/mmc$ (red line) and $R\bar{3}m$ symmetry (green line).

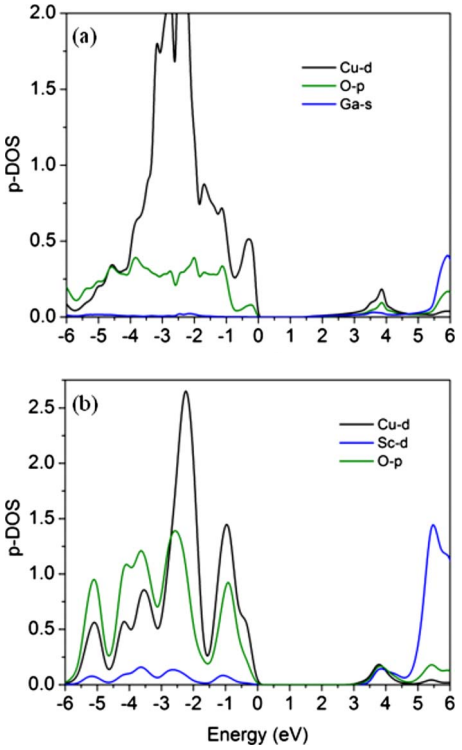

FIG. 3. (Color online) Two representative partial DOS plots are shown: (a) rhombohedral $CuGaO_2$ and (b) hexagonal $CuScO_2$.

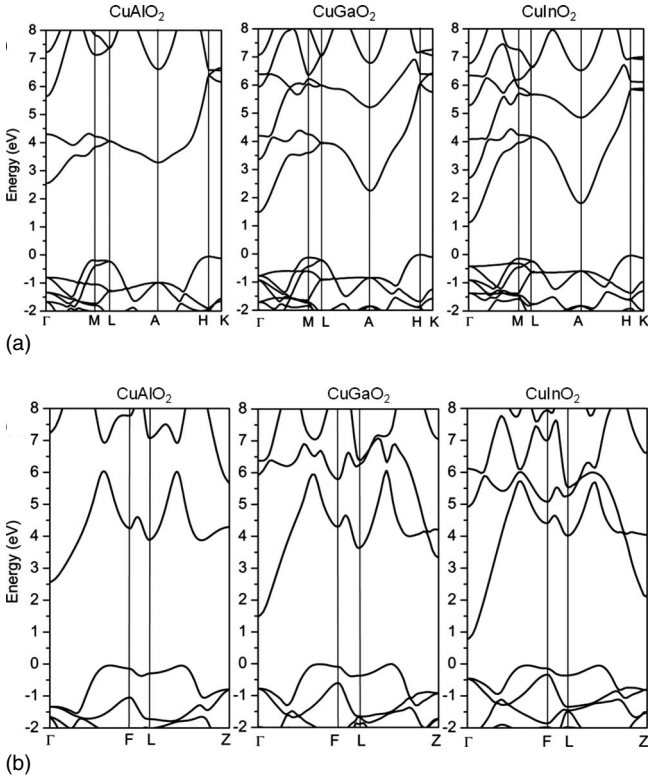

FIG. 4. Calculated electronic band structure of (a) hexagonal and (b) rhombohedral group-IIIA delafossites along the high-symmetry lines of the first Brillouin zone.

chemical in nature rather than structural. From Figs. 2(a) and 2(b), we see that for both $CuAlO_2$ and $CuGaO_2$, the hexagonal and rhombohedral symmetries have similar DOS features near the top of the valence band, which is most important for *p*-type conductivity. Figure 3 shows the orbital projected partial density of states (p-DOS) for two representative cases: (a) from group IIIA, rhombohedral $CuGaO_2$ and (b) from group IIIB, hexagonal $CuScO_2$. For example, from Fig. 3(a), the presence of an unoccupied Ga *s* band is seen around 6 eV above the Fermi level and a long *s*-band tail at the bottom of the conduction band is observed in Fig. 2(b). The Ga *d* band has a very minor contribution to the upper valence band due to its high binding energy. On the other hand, due to the higher energy of the unoccupied Al *s* band, its contribution lies outside the scale of the DOS plot as shown in Fig. 2 and 3.

The question can now be asked, *why does group IIIA stabilize in the rhombohedral structure, whereas group IIIB stabilizes in the hexagonal structure*? In comparison with $CuGaO_2$ or $CuInO_2$, the presence of barely filled 3*d* states due to Sc appears to have more influence on the valence-band structure between the two structures for $CuScO_2$ [Fig. 2(c)]. The electron density of $CuScO_2$ at the Fermi level has a more pronounced and localized peak for the rhombohedral symmetry than that of the hexagonal one. This type of high DOS near the Fermi level may be responsible for its structural transition from rhombohedral to a relatively lower symmetry hexagonal structure. This transition is possible due to the lower symmetry of hexagonal structures, which results in some extra hybridization between the unoccupied Sc *d* and occupied O *p* levels. This type of hybridization is not possible in the rhombohedral structure due to the symmetry constraints. So, the level repulsion in rhombohedral structure results in higher DOS near the Fermi level. On the other hand, for the hexagonal structure, the total DOS peak moves away slightly from the Fermi level [Fig. 2(c)] due to the above-mentioned band coupling. Group-IIIA delafossites do not show this transition because of the lack of unoccupied *d* bands near the Fermi level from group-IIIA atoms. In the case of this type of transition (rhombohedral to hexagonal) because the *p*-*d* orbital energy difference is relatively large, the energy gain is not significant. We have also calculated the Madelung energy in both cases to see if the electrostatic energy has any role in determining the symmetry of the delafossites, as it does in the case of ZnO. In ZnO, the hexagonal wurtzite structure is stabilized over the cubic zinc-blende phase due to the gain in the electrostatic energy.[26] However, for the delafossite system, the electrostatic energy difference between the two structures is negligible.

B. Band structures

We now discuss the electronic band-structure differences between the $CuM^{IIIA}O_2$ and $CuM^{IIIB}O_2$ families. Figure 4 shows the band structures for the $CuM^{IIIA}O_2$ family with the (a) hexagonal and (b) rhombohedral structures. Similarly, Fig. 5 contains the band structure for the $CuM^{IIIB}O_2$ family delafossites. The calculated band structures for the rhombohedral $CuM^{IIIA}O_2$ family can be compared with the previously published band structure calculated by the local-

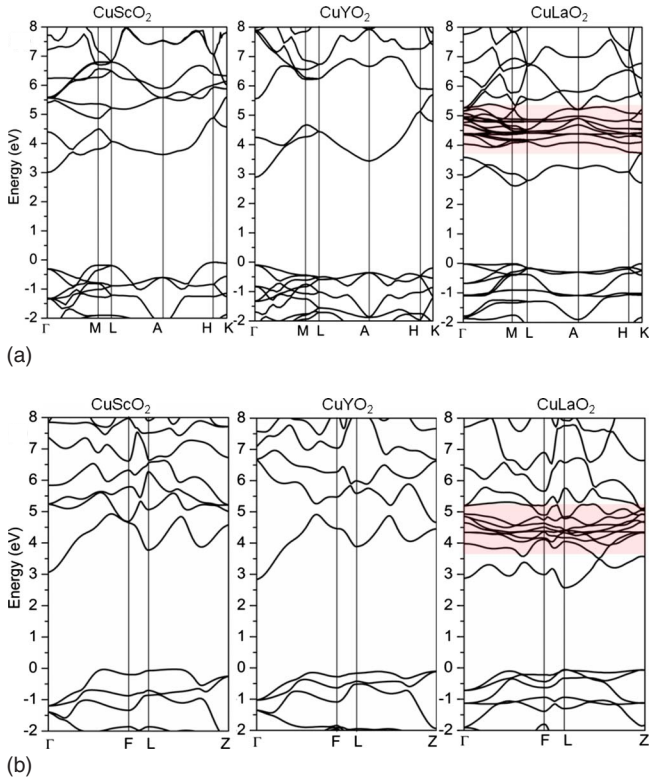

FIG. 5. (Color online) Calculated electronic band structure of (a) hexagonal and (b) rhombohedral group-IIIB delafossites. The shaded areas for $CuLaO_2$ indicate the presence of La f band in the conduction bands.

density approximation (LDA)-DFT Hamiltonian without any U parameter.[12] Comparing Figs. 4(a) and 4(b), we see that although the details of the band structure somehow differ, the overall similarity at the band edges is quite clear. For example, the direct band gap at Γ point is about the same for both symmetries for group-IIIA delafossites. Also, for this group (Fig. 4), we see a gradual lowering in energy of the CBM s-like state [such as shown in the p-DOS plot for $CuGaO_2$ in Fig. 3(a)] at Γ point from Al to Ga to In. The main reason for the very low fundamental band gap (indirect) in this group of delafossites is the presence of this extended s band. Also, the successive rise of the valence-band edges at Γ point (with respect to the VBM) was seen as one goes from Al to Ga to In. The top of the valence band (VBM) occurs at the H point for hexagonal symmetry. For rhombohedral symmetry, this is equivalent to a point between the Γ and F points, as was also found in Ref. 12, and the direct gap at this point is more than 5 eV. However, the conduction-band edge at the H point (for hexagonal) lowers slightly (by about 0.7 eV) going from Al to In. At this point, the conduction band has mainly s-p (with more p) character, whereas the valence band has p-d (with more d) character. So, optical absorption at this point is possible but in the ultraviolet region. It is also quite clear that the CBM is highly dispersive and relatively low in energy, especially for the In compound. So, in principle, n-type doping should be possible in $CuInO_2$ materials.

Comparing the band structures for the $CuM^{IIIA}O_2$ and $CuM^{IIIB}O_2$ delafossites, we find that the nature of the valence band is similar for both group-IIIA and IIIB families. As mentioned earlier, and as can be seen from Figs. 3(a) and 3(b), the VBMs are mainly composed of Cu d and O p orbitals. Also, the contribution of the d band from the metal M atoms (M=Sc, Y, or La) in the VBM is not very significant, other than that it helps to stabilize the hexagonal structure. For example, Fig. 3(b) shows that the contribution of Sc d at VBM is negligible. However, for hexagonal $CuM^{IIIB}O_2$ band structures [Fig. 5(a)], the occurrence of the VBM at the H point is no longer found in all cases. For example, for $CuScO_2$, the VBM is still at the H point but for $CuYO_2$ and $CuLaO_2$, the VBM is at the Γ point. In $CuYO_2$, the valence band at the H point has significant Cu s mixture, whereas the conduction band at this point has a good contribution from Y d band. Also, the position of the top of the valence band at the Γ point relative to the VBM is not the same for a given group-IIIB delafossite for the two structures, unlike the group-IIIA delafossites. The extent of hybridization of O p and M^{IIIB} d plays an important role in this. Nevertheless, the slight uplift of valence band at the Γ point is seen from Sc to Y to La with respect to the VBM.

Larger variations are seen between the CBM of the group-IIIA and group-IIIB delafossites. The biggest difference is that at the Γ point, the s-band-derived CBM in the $CuM^{IIIB}O_2$ family is not as deep as compared to that in the $CuM^{IIIA}O_2$ family. First, comparing the band structure of $CuScO_2$ and $CuGaO_2$, we clearly see the much lower CBM due to the Ga 4s band in the later at the Γ point. This is also indicated in Figs. 3(a) and 3(b). For $CuScO_2$, the presence of unoccupied Cu 3d states at the CBM (Γ point) makes it much less dispersive. Second, for Ga, all its 3d bands are occupied and are situated at much higher binding energy below the Fermi level; therefore, they do not contribute much to the conduction band. At the L point (second-lowest CBM for rhombohedral symmetry where the optical absorption is much higher[12]), significant Ga s contribution along with p character is seen for $CuGaO_2$. In contrast, for $CuScO_2$, the d contribution is significant at the L point of the conduction band because of its partially filled Sc 3d nature. In addition, unoccupied f bands are present in the conduction band in $CuLaO_2$ that affect the CBM significantly. The La f bands in the conduction bands are indicated by the shaded box in Fig. 5(b).

In principle, all the differences identified above can be attributed to the differences in electronic configurations between group-IIIA and IIIB elements. For example, the 4s (Sc), 5s (Y), and 6s (La) orbitals are shallower than their corresponding 3d (Sc), 4d (Y), and 5d (La), whereas the 3p (Al), 4p (Ga), and 5p (In) are relatively shallower than their corresponding s bands, and group IIIA does not have unfilled d bands near the band edges. Among all the M elements, only La involves f orbitals. These differences create significant changes to the band-gap trends between the $CuM^{IIIA}O_2$ and $CuM^{IIIB}O_2$ families, as discussed in more detail below.

C. Trends in the band gaps

For the band-gap discussion, we mainly consider the most-stable phase for the two delafossite families presented

here, i.e., hexagonal for group IIIB and rhombohedral for group IIIA. The higher position of CB at the Γ point relative to the VBM for Cu$M^{\mathrm{IIIB}}O_2$ family leads to a much decreased difference between the indirect and direct band gaps as compared with the Cu$M^{\mathrm{IIIA}}O_2$ family. Here, the indirect band gap or the fundamental band gap is defined as the smallest gap between the VBM and CBM over all **k** points. For group IIIB, experimentally the measured optical band gaps are 3.7,[17] 3.5,[18] and 2.4 (Ref. 19) eV for $CuScO_2$, $CuYO_2$, and $CuLaO_2$, respectively. Without a Hubbard U parameter in the GGA Hamiltonian, the calculated smallest indirect gaps are 2.25, 2.62, and 2.62 eV for $CuScO_2$, $CuYO_2$, and $CuLaO_2$, respectively. For the less-preferred rhombohedral structure, the smallest indirect band gaps were 2.27, 2.67, and 2.61 eV for $CuScO_2$, $CuYO_2$, and $CuLaO_2$, respectively. These band gaps are smaller than the experimental values and the trends are also inconsistent with the experimental results. The differences in trends are because the LDA/GGA band-gap error for the occupied 3d band is much larger in energy than 4d and 5d bands. Corrections to these d bands could restore the band-gap trend for the group-IIIB delafossites. For $CuScO_2$, $CuYO_2$, and $CuLaO_2$, the modified smallest band gaps with DFT+U were found to be 3.09, 2.93, and 2.63 eV, respectively, for the hexagonal cell. The band-gap difference between $CuScO_2$ and $CuYO_2$ is 0.16 eV, comparable to their experimental band-gap difference of 0.20 eV. The calculated direct band gap at the Γ point is 3.31 eV for $CuScO_2$. The difference between the direct and indirect gaps for $CuScO_2$ is only 0.22 eV. Such a small difference is not easy to detect experimentally with linear fits to optical-absorption data. This is likely the reason why all optical measurements have revealed a direct band gap for $CuScO_2$.

For $CuYO_2$, the Y 4d bands are relatively more delocalized than 3d. To check the effect of U on 4d, we considered two cases, U=4.0 and 7.0 eV. In both cases, the band gap remains direct at the Γ point for $CuYO_2$. The reason is that for relatively large U, the CBM at the Γ point has mostly s character and the VBM has mostly the O p and Cu d character, which is not very sensitive to the U applied to Y 4d. Higher VBM values in group-IIIB delafossites have been obtained by band-offset calculations in a recently published study.[27] In fact, the relative contribution from Cu d at VBM increases as one goes from Sc to Y to La. Also, as the lattice parameter in the ab plane increases significantly from Sc to La, the interchain interaction for the Cu-O chain reduces and leads to a less dispersive (almost flat-shaped band) VBM with major Cu d contributions. Although it may mean higher effective mass for the holes, appropriate band engineering by isovalent alloying may improve this situation.[28] It is also interesting to note that although the average Cu-O distance in group-IIIA delafossites is 1.83 Å, the average Cu-O distance for the group-IIIB delafossites is slightly less than 1.80 Å. This also indicates a higher overlap of Cu d and O p wave functions for group-IIIB delafossites. This leads to stronger hybridization and higher bonding-antibonding splitting. This effect is prominent for the less-symmetric hexagonal structures. On a similar ground, due to the presence of La 5f bands, $CuLaO_2$ also showed direct band gaps because the Γ point no longer remains as the CBM. It shows clearly that the difference between the direct and indirect band gaps, wherever is exists, is significantly smaller for the Cu$M^{\mathrm{IIIB}}O_2$ family than for the Cu$M^{\mathrm{IIIA}}O_2$ family.

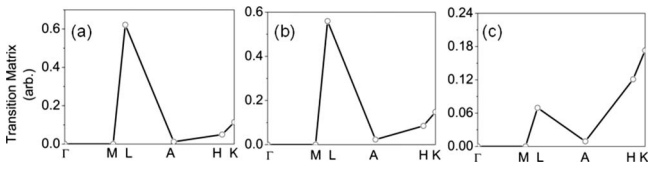

FIG. 6. The optical transition probabilities (here represented by the dipole transition matrix) from the highest valence band to the lowest conduction band are shown for group-IIIB delafossites: (a) $CuScO_2$, (b) $CuYO_2$, and (c) $CuLaO_2$. The probabilities are only shown at the special **k** points for hexagonal symmetry, which is the stable phase for this delafossite group. The lines are guides to the eyes only.

D. Optical transition probability

We have also calculated the optical transition matrix elements for the band edges of group-IIIB delafossites (Fig. 6) at the special symmetry points, as shown in the band structure in Fig. 5(a).[29] These matrix elements were calculated by the optic code[30] as implemented in WIEN2K.[31] Here, only the diagonal components (direct gap) of the momentum matrix were calculated because the off-diagonal elements would not contribute significantly to strong optical absorption. For all cases in Fig. 6, the transition between VBM and CBM at the Γ point is forbidden (zero transition matrix elements) because of the mainly d character for both VBM and CBM and the transition would result in a parity violation. Unlike oxides such as ZnO (Ref. 5) or WO_3,[32] such parity-forbidden transitions resulting in an inequivalence in the optical and fundamental band gaps also found in other oxide systems, for example, in In_2O_3 (Ref. 33) or in spinel Cd_2SnO_4.[34] As is seen from Fig. 6, for $CuScO_2$ and $CuYO_2$, transition matrix elements show stronger absorption at the L point where the direct gaps are more than 3.5 eV. The reason for higher transition probability is that, at this point, the CBM has higher p contribution and VBM has mainly d contribution, so p-d transition is favorable here. It is clear from this high-energy L-point transition that with a relatively higher band gap, $CuScO_2$ and $CuYO_2$ should be better TCOs if good conductivity can also be achieved. On the other hand, $CuLaO_2$ shows a different behavior because of the presence of a highly localized unfilled f band near the CBM. It shows higher adsorption at H and K points, and the L-point transition is suppressed. Due to the lower band gap, $CuLaO_2$ should be a better candidate as a photoelectrode for PEC hydrogen production than other Cu delafossites. However, the weak absorption near the band-gap energy is still an issue and should be addressed.

IV. CONCLUSIONS

In conclusion, our first-principles calculations have revealed that although the Cu$M^{\mathrm{IIIA}}O_2$ and Cu$M^{\mathrm{IIIB}}O_2$ delafossites have similar local structure environment, they have very different electronic properties. We found that these differ-

ences can be explained by the different atomic configurations between the group-IIIA and IIIB elements. We found that group-IIIA and IIIB delafossites stabilize in rhombohedral and hexagonal structures, respectively. We present an explanation for why the hexagonal phase of group-IIIB delafossites is stabilized over the rhombohedral one. Our study revealed that this is due to the extra coupling between the occupied O p and unoccupied M^{IIIB} d bands in hexagonal symmetry, which is otherwise not possible in higher symmetric rhombohedral structures. Group-IIIA delafossites do not show this structural transition because the M^{IIIA} d bands are either fully occupied (Ga and In) or completely unoccupied at very high energy (Al). Our results explain well the experimentally reported band-gap trends for $CuM^{\mathrm{IIIB}}O_2$ delafossites and they indicate that although $CuScO_2$ and $CuYO_2$ could be excellent candidates for p-type TCOs, $CuLaO_2$ would be better for the photoelectrodes of PEC hydrogen production. These understandings also provide insight on the physics of wide band-gap semiconductors regarding their applicability in optoelectronic devices in general.

ACKNOWLEDGMENTS

M.N.H. gratefully acknowledges the fruitful discussions with Eric W. McFarland and John A. Turner. This work was supported by the U.S. Department of Energy under Contract No. DE-AC36-08GO28308. This research used resources of the National Energy Research Scientific Computing Center, which is supported by the Office of Science of the U.S. Department of Energy under Contract No. DE-AC36-08GO28308.

*muhammad.huda@nrel.gov

[1] O. Khaselev and J. A. Turner, Science **280**, 425 (1998).
[2] M. Grätzel, Nature (London) **414**, 338 (2001).
[3] A. Fujishima and K. Homda, Nature (London) **238**, 37 (1972).
[4] T. Bak, J. Nowotny, M. Rekas, and C. C. Sorrell, Int. J. Hydrogen Energy **27**, 991 (2002).
[5] M. N. Huda, Y. Yan, S.-H. Wei, and M. M. Al-Jassim, Phys. Rev. B **78**, 195204 (2008).
[6] M. Younsi, S. Saadi, A. Bouguelia, A. Aider, and M. Trari, Sol. Energy Mater. Sol. Cells **91**, 1102 (2007).
[7] S. Saadi, A. Bouguelia, A. Derbal, and M. Trari, J. Photochem. Photobiol., A **187**, 97 (2007).
[8] H. Kawazoe, M. Yasukawa, H. Hyodo, M. Kurita, H. Yanagi, and H. Hosono, Nature (London) **389**, 939 (1997).
[9] I. Hamberg and C. G. Granqvist, J. Appl. Phys. **60**, R123 (1986).
[10] C. G. Granqvist and A. Hultaker, Thin Solid Films **411**, 1 (2002).
[11] A. Buljan, M. Llunell, E. Ruiz, and P. Alemany, Chem. Mater. **13**, 338 (2001).
[12] X. Nie, S.-H. Wei, and S. B. Zhang, Phys. Rev. Lett. **88**, 066405 (2002).
[13] J. Pellicer-Porres, A. Segura, A. S. Gilliland, A. Muñoz, P. Rodríguez-Hernández, D. Kim, M. S. Lee, and T. Y. Kim, Appl. Phys. Lett. **88**, 181904 (2006).
[14] S. Gilliland, J. Pellicer-Porres, A. Segura, A. Muñoz, P. Rodríguez-Hernández, D. Kim, M. S. Lee, and T. Y. Kim, Phys. Status Solidi B **244**, 309 (2007).
[15] B. J. Ingram, G. B. Gonzalez, T. O. Mason, D. Y. Shahriari, A. Barnabe, D. Ko, and K. R. Poeppelmeier, Chem. Mater. **16**, 5616 (2004).
[16] M. S. Lee, T. Y. Kim, and D. Kim, Appl. Phys. Lett. **79**, 2028 (2001).
[17] Y. Kakehi, K. Satoh, T. Yotsuya, K. Masuko, and A. Ashida, Jpn. J. Appl. Phys. **46**, 4228 (2007).
[18] M. Trari, A. Bouguelia, and Y. Bessekhouad, Sol. Energy Mater. Sol. Cells **90**, 190 (2006).
[19] N. Koriche, A. Bouguelia, and M. Trari, Int. J. Hydrogen Energy **31**, 1196 (2006).
[20] J. P. Perdew, J. A. Chevary, S. H. Vosko, K. A. Jackson, M. R. Pederson, D. J. Singh, and C. Fiolhais, Phys. Rev. B **46**, 6671 (1992).
[21] P. E. Blöchl, Phys. Rev. B **50**, 17953 (1994).
[22] G. Kresse and D. Joubert, Phys. Rev. B **59**, 1758 (1999).
[23] G. Kresse and J. Hafner, Phys. Rev. B **48**, 13115 (1993); G. Kresse and J. Furthmüller, Comput. Mater. Sci. **6**, 15 (1996); G. Kresse and J. Furthmüller, Phys. Rev. B **54**, 11169 (1996).
[24] T. Ishiguro, N. Ishizawa, N. Mizutani, and M. Kato,J. Solid State Chem. **49**, 232 (1983).
[25] B. J. Ingram, T. O. Mason, R. Asahi, K. T. Park, and A. J. Freeman, Phys. Rev. B **64**, 155114 (2001).
[26] S. Takeuchi and K. Suzuki, Phys. Status Solidi A **171**, 99 (1999).
[27] L.-J. Shi, Z.-J. Fang, and J. Li, J. Appl. Phys. **104**, 073527 (2008).
[28] For the group-IIIA delafossite optical transition matrix elements please see Ref. 12. Also, optical transition probabilities of $CuAlO_2$, $CuScO_2$, and $CuYO_2$ in rhombohedral symmetry are given in Ref. 27. It should be mentioned here that in these previous calculations no U was added in the Hamiltonian, so the extent of d hybridization at CBM would differ from the present calculation. This would also lead to slightly different transition probabilities for calculations with and without U.
[29] M. N. Huda, Y. Yan, A. Walsh, S.-H. Wei, and M. M. Al-Jassim, Appl. Phys. Lett. **94**, 251907 (2009).
[30] C. Ambrosch-Draxl and J. O. Sofo, Comput. Phys. Commun. **175**, 1 (2006).
[31] P. Blaha, K. Schwarz, G. K. H. Madsen, D. Kvasnicka, and J. Luitz, *WIEN2K, An Augmented Plane Wave + Local Orbitals Program for Calculating Crystal Properties* (Techn. Universität Wien, Austria, 2001).
[32] M. N. Huda, Y. Yan, C.-Y. Moon, S.-H. Wei, and M. M. Al-Jassim, Phys. Rev. B **77**, 195102 (2008).
[33] A. Walsh *et al.*, Phys. Rev. Lett. **100**, 167402 (2008).
[34] D. Segev and S.-H. Wei, Phys. Rev. B **71**, 125129 (2005).